

FAULT SLIP IN A MINING CONTEXT

N.D. Fowkes*, D.P. Mason† and J.A.L. Napier‡

Abstract

Recent articles on the broad range of computational and analytic techniques currently used to investigate excavation collapse are reported. Advances in physical models are also described. Simple models for determining fault slip due to underground and surface excavations and structures are investigated.

1 Introduction

Fault line slip can result in excavation collapse and so is a major safety concern for miners. Such slip can be brought about by seismic activity remote from the mining site or can be locally generated by the mining activity itself; the latter is of primary concern here. Underground excavations may cause a reduction in the normal force acting on a nearby fault or increase the shearing force acting along the fault and thus result in fault line slip. Furthermore the effect of slip along fault will cause a redistribution of stress throughout the mining site so that other faults may slip or may be further loaded; subsequent mining activity may trigger such faults. The failure may be static in character in the sense that a quasi-steady description of the stress field can be used to identify unsafe faults, or dynamic in the sense that elastic wave propagation issues need to be taken into account. Further complications arise in that very little relevant information is available about the geology and stress state of the mining area, and it is unlikely that such information will ever be practicably available. The problem is very difficult

*School of Mathematics and Statistics, University of Western Australia, Crawley WA 6009 Australia, *e-mail: fowkes@maths.uwa.edu.au*

†School of Computational and Applied Mathematics and Centre for Differential Equations, Continuum Mechanics and Applications, University of the Witwatersrand, Private Bag 3, Wits 2050, Johannesburg, South Africa, *e-mail: dpmason@cam.wits.ac.za*

‡School of Computational and Applied Mathematics, Private Bag 3, Wits 2050, Johannesburg, South Africa, *e-mail: jnapier@cam.wits.ac.za*

both because the physics is not well understood and because of the absence of data.

One might well argue that the objective of collecting sufficient data to allow rigorous modelling is futile given the complex nature and large variability of materials and site conditions. Generally, however, it is agreed that models should be seen as a numerical laboratory where the engineer experiments with the main variables and parameters, learning about their mutual relations and their influence on global behaviour; this approach has been adopted by the Division of Mining Technology, CSIR, South Africa. Many person years have been invested in trying to understand how to deal with the physics and numerics of this problem. Recent articles on the broad range of computational and analytic techniques currently used in the area, and advances in physical models and hazard assessment have been presented here. These results are taken primarily from review articles presented in *Advances in Geophysics in the seismic and mining context*, see Panza, Romanelli and Vaccari (2000), King and Cocco (2000), and Gibowicz and Lasocki (2000). As indicated we are primarily concerned with the effect of mining activities on the structural integrity of excavations. Mines are normally built in locations containing faults and the effect of removing rock from the mining site is to change the loading on nearby faults, possibly causing slip. Also vibrations induced by mining operations generate elastic waves that can cause slip on faults or movement of excavation walls, resulting in collapse. Generally it is assumed that failure initiates and spreads on the fault plane if the Coulomb Failure Function C_f exceeds a specific (experimentally determined) value:

$$C_f = |\tau_\beta| + \mu\sigma_\beta, \quad (1.1)$$

where τ_β, σ_β are the shear stress and normal stress (positive for extension) acting on the fault orientated at angle β and μ is the coefficient of friction. This result can be expressed in terms of the principal stresses and, using this, optimal slip planes simultaneously favoured by initial loading and orientation, can easily be identified, see King and Cocco (2000). This greatly simplifies the task of predicting slip. When used in combination with the momentum balance equation for elastic media,

$$\rho u_{i,tt} = \rho F_i + \tau_{ij,j},$$

where F_i is the body force per unit mass, τ_{ij} is the Cauchy stress tensor, u_i the displacement vector, and the constitutive relation

$$\tau_{ij} = f_{ij}(u_{r,s}),$$

for the material, and appropriate boundary and initiating conditions, one can, in theory, determine slip under prescribed forcing. Note that:

- The constitutive law is problematic. The elastic behaviour is likely to be determined primarily by micro and macro cracks (rather than by the intact rock) and is likely to vary with location especially close to fault zones. Furthermore the effect of previous seismic events is to change shear stress levels in the neighbourhood of faults, see later.
- The failure condition is simplistic, see later.
- Elastic waves are complex in their own right and their interaction with structures adds further complications. Both shear and pressure waves are generated by disturbances with the energy apportionment dependent on the source characteristics and the presence of boundaries. Whether or not a fault slips depends on the nature and strength of the stress wave, its direction of propagation, and the orientation and state of loading of the fault.

We shall now describe some of the approaches used to better understand these issues.

1.1 More complex failure models: memory

Both rate and state dependent failure laws have been proposed to explain the occurrence and timing of aftershocks. Such models may be thought to be associated with a slip-stick phenomena or some types of viscoelastic relaxation process, although it is perhaps best to just think of such models as being purely empirical and requiring laboratory fitting. In the context of fault failure it is necessary to take into account changes in the status of the fault brought about by previous seismic activity, and the introduction of a memory (hysteresis) state variable θ , dependent on the past history of the slip velocity V , represents a simple fix. Generally two coupled equations are introduced; the *governing equation*, which determines the sliding resistance τ to the slip velocity V . A typical form used is

$$\tau = \mu\sigma_n + A \ln \frac{V}{V^*} + B \ln \frac{\theta}{\theta^*},$$

and a second equation

$$\theta_t = F(\theta, L, V),$$

which determines the change in the memory variable θ , see Dieterich (1996). Apart from the normal Coulomb terms there are slip velocity and state dependent terms with cut off values (V^*, θ^*) included; all introduced parameters (A, B, θ^*, V^*) would need to be measured or fitted. Additionally F needs to be modelled. Such equations have been used to model earthquake after-effects including stress triggering. It should be pointed out, however, that in the fault context simple laws of the above type are far from satisfactory and models taking into account crack opening have been suggested, see Napier and Malan (1997), and Dyskin and Galybin (2004).

1.2 Other Features

Numerical simulations suggest that seismic ground motion is greatly amplified on mountain tops and strongly dependent on the incidence angle and sharpness of the topography. Also the trapping of energy due to soft surface layering above underlying rock plays an important role in many situations as well as resonances associated with the topology. Apart from fault zone relaxation effects there are long term stress redistribution (aseismic creep or flow) effects that change the loading on faults.

1.3 Self organised criticality

It would appear that very small changes in the Coulomb stress levels (0.1 -1 bar) can influence the occurrence of future earthquakes which have associated stress drops of the order of several bars to hundreds of bars, see King and Cocco (2000). It has been suggested that faults behave as a *self-organised critical system*; under such circumstances even small stress changes can produce an instability. Furthermore some researchers believe that much of the earth's crust is not far from instability and provide data to support this view. Some non-linear elastic models, see Muhlhaus (1999) predict 'give' in layers sandwiched between intact layers in response to shear; essentially strain concentrations tend to be concentrated in zones. Such models perhaps might be used to explain fault behaviour and in particular the observed self criticality in stressed areas. These models are chaotic in behaviour; small changes in the initial or boundary conditions can strongly affect the location of the layers of give.

A surprisingly strong seismic response to small changes in the Coulomb stress levels is also observed in the mining context where almost all the seismic activity is induced by mining excavations, see Gibowicz and Lasocki (2000). Many small scale seismic events (up to order of 100 per year) are

recorded with a very small proportion causing rock failures. Comprehensive studies of such events have been carried out in South Africa, Poland, Canada and the United States

Based on these observations we will suggest another way forward, see Section 3.

2 Summary of mathematical techniques

2.1 Numerical techniques

Useful analytic results (ray tracing and mode coupling) are available in cases in which the wavelength of the seismic signal (typically 100m) greatly exceeds the dimensions of lateral heterogeneities; evidently not the case in the mining context. Crude analytic approaches may well be useful for identifying critical parameter combinations but to date researchers have relied on numerical procedures. Of the standard techniques finite difference and finite element techniques require huge amounts of memory and CPU time, pseudo-spectral methods require rather less. Setting up an accurate finite difference scheme on other than a Cartesian grid can be achieved using a local mapping function but this quickly becomes unmanageable for even simple fault arrangements. The finite element technique better handles the awkward geometries associated with the fault configuration and mine geometry. For the linear constitutive model standard boundary integral techniques can be used, greatly reducing the memory requirements and CPU time, providing the material parameters are uniform. Awkward geometries can be handled with care.

More promising perhaps than the above are fault interaction models, see King and Cocco (2000). The approach, a boundary integral approach, makes use of the static Green's function solution for the displacement in an infinite elastic isotropic and homogeneous half space due to a volume point force of prescribed orientation. Excavations and faults are represented as slip planes with prescribed displacements determined so that a consistent picture results; simultaneous solutions of the governing boundary integral equations for the fault displacements are sought. Evidently the problem of discretization of the complete space is avoided and the technique focuses on the most important issues (assuming the elastic field is essentially homogeneous except near faults).

Another procedure that has been successfully used for extremely complex problems of an industrial origin is the particle interaction model, see Cleary and Ha (2001). The technique was originally used by Monaghan (1992) in

an astrophysics context. The continuum is viewed as a collection of moving discrete particles interacting across their boundaries. Either the interaction is described in terms of simple, often empirical (hard particle) models of a dash-pot spring type, or the continuum equations are averaged to determine the interaction (smooth particle models). It is a simple matter with the hard particle models to account for state changes of individual particles so that in the present context memory effects would be easily handled. Also the hard particle models do not make any great distinction between liquids and solids (except through the interaction) so that interfaces of all types are easily handled. These methods are basically ‘zero order’ methods and so are not efficient in a technical sense, although one has to add that conventional techniques are not easily able to handle complex situations and lose accuracy¹ in circumstances in which the techniques have been successfully applied (eg. free surface problems).

2.2 Statistical and semi-statistical techniques

The ideas presented above represent attempts to use our understanding of the physics to predict behaviour. Given the complexity a pessimist might conclude that all such attempts are likely to fail and that a statistical approach is the way to go, and of course all manner of deterministic/statistical combinations have been used. Seismic zoning using scientific data banks integrated in an expert system have been used to identify suitable areas for urban development as well as to mark out regional hazard zones, see Panza, Romanelli and Vaccari (2000). Such models have used data concerning the area, combined with synthetic seismograms, to estimate ground accelerations resulting from events. Also of course in the mining context a great deal of information² is readily collected at a mine site so that a temporal and spatial pattern of activity and its relation to the source can be established. The available results are often sufficient to determine variations of wave speed so that parameter maps can be constructed. A variety of source parameters (seismic moment, corner frequency, energy flux) are extracted from spectral data collected from carefully designed seismic networks recording hundreds of events per day. In order to collapse data into a useful form various scaling relations connecting the above parameters have been used, and also fractal relations connecting the observed size and spatial and temporal patterns of seismic events have been suggested. The indications are that a fractal description (of small dimension) works, which suggests that

¹as seen in a reduction in order

²many events per day is not unusual

rock fracturing may be governed by a simple deterministic but chaotic set of equations. Linear and non-linear statistical extrapolation models have been suggested. The above description is brief, for more information see Gibowicz and Lasocki (2000).

3 Simple 2D fault slip models

If the observed seismic events are a direct consequence of the critically stressed state of a mining site before the events, then it seems sensible to primarily focus one's attention on the pre-event state, appending perhaps a stability analysis. The determination of the change in the *static* field brought about by the mining works is thus seen to be the essence of the problem. The actual stress state corresponding to a specific mining configuration at the present time would be independent of previous history providing there has been no slippage³. Once slip has occurred, however, a historic record needs to be kept and a simple fault slip model would be necessary to determine future developments.

The vertical component of the ambient stress is primarily due to the overburden, whereas tectonic forces can affect the horizontal ambient stresses. A small redistribution of such large loading, brought about by rock removal, could well lead to catastrophic collapse. (A heavy beam supported by vertical struts subject to movement comes to mind). If the above image is correct then one should focus ones attention on build up of stress away from ambient brought about by the removal of rock in the presence of known faults; a perturbation approach is indicated.

Simple exact solutions are available in the plane stress case; we will use these results to illustrate the envisaged procedure. Following Timoshenko and Goodier (1970): in regions excluding excavations and faults the equations of static equilibrium and the compatibility equation are

$$\tau_{xx,x} + \tau_{xy,y} = 0, \quad (3.1)$$

$$\tau_{yy,y} + \tau_{yx,x} - \rho g = 0, \quad (3.2)$$

$$\nabla^2(\tau_{xx} + \tau_{yy}) = 0. \quad (3.3)$$

The x axis is horizontal, the y axis vertically upwards, and the origin a point on the surface, as in Figure 1.

³assuming a linear model

Consider first the ambient stress state, τ_{ik}^0 , before excavations have been initiated. The surface $y = 0$ is traction-free. Equations (3.1) to (3.3) and the traction-free boundary condition are satisfied by

$$\tau_{xx}^0 = \tau_{xx}^0(y), \quad \tau_{yy}^0 = \rho gy, \quad \tau_{xy}^0 = 0,$$

provided

$$\frac{d^2}{dy^2} \tau_{xx}^0 = 0.$$

The theory of elasticity gives no clear indication as to what the horizontal stress τ_{xx}^0 should be (Jaeger and Cook, 1969). Many authors take

$$\tau_{xx}^0 = k \tau_{yy}^0 = k \rho gy, \quad 0 < k < 1,$$

where k is a constant. The case $k = 0$ corresponds to no lateral constraint ($\tau_{xx}^0 = 0$). If there is no horizontal displacement anywhere ($u_x = 0$) then it follows from the generalised Hooke's law that

$$\tau_{xx}^0 = \frac{\nu}{1 - \nu} \tau_{yy}^0,$$

where ν is the Poisson ratio. For a Poisson material, for instance, $\nu = \frac{1}{4}$. Then

$$\tau_{xx}^0 = \frac{1}{3} \tau_{yy}^0$$

and $k = \frac{1}{3}$. When $k = 1$,

$$\tau_{xx}^0 = \tau_{yy}^0 = \rho gy, \quad \tau_{xy}^0 = 0.$$

The stresses are then described as lithostatic. The assumption that the stresses at depth are lithostatic is referred to as *Heim's rule* (Jaeger and Cook, 1969). Heim stated that stresses in rock tend to become lithostatic due to creep. Because stresses in sediments are lithostatic throughout the process of rock formation it can be argued that the final state of stress in the rock should also be lithostatic.

In order to gain insight into the fault slip behaviour we will take a simplified approach and choose $k = 0$:

$$\tau_{xx}^0 = 0, \quad \tau_{yy}^0 = \rho gy, \quad \tau_{xy}^0 = 0.$$

An extension of this work would be to consider the case $0 < k \leq 1$. Changes in stress τ'_{ij} away from from ambient thus satisfy

$$\tau'_{xx,x} + \tau'_{xy,y} = 0, \tag{3.4}$$

$$\tau'_{yy,y} + \tau'_{xy,x} = 0, \quad (3.5)$$

$$\nabla^2(\tau'_{xx} + \tau'_{yy}) = 0. \quad (3.6)$$

Such changes are brought about by forces effectively applied around exposed surfaces; faults, excavations and the free surface. The solutions of the equations (3.4, 3.5) can be developed in terms of the Airy stress function ϕ with

$$\tau'_{xx} = \phi_{yy}, \quad \tau'_{yy} = \phi_{xx}, \quad \tau'_{xy} = -\phi_{xy}, \quad (3.7)$$

and the compatibility equation (3.6) then yields

$$\nabla^4\phi = 0. \quad (3.8)$$

In the present context we need solutions of the biharmonic equation suitable for representing faults and excavations. Relevant singular solutions for ϕ in local cylindrical co-ordinates (r, θ) are the point source solution $r\theta \cos \theta$ and the edge dislocation solution θ . Other biharmonic solutions may need to be appended to generate the required exact solutions.

A number of excavation and fault arrangements have been examined, a few of which will be reported here.

3.1 Fault slip due to an excavation above a fault

We determine the effect of drilling an excavation of radius a above (and parallel to) a fault orientated at an angle β to the Earth's surface. It is convenient to prescribe the excavation's location using the distances (d, H) , see Figure 1; d is the perpendicular distance of the excavation from the fault and H provides a measure for the depth of the excavation⁴. Locations along the fault are conveniently measured using the angular displacement α as measured away from the normal to the fault from the excavation, see Figure 1. The primary effect of the excavation is to introduce a point force

$$\mathbf{P} = P\mathbf{j} = \pi a^2 \rho g \mathbf{j} \quad (3.9)$$

per unit length acting vertically upwards on the surrounding material. For simplicity we will use the expression for a point force in an *infinite* medium; we should use the expression for a point force in a *half plane*. Our solution will give rise to nonzero normal and shear stresses at the surface, which however will be small for deep excavations; explicitly $d/H \ll 1$ is required for

⁴the excavation depth is $H - d \cos \beta$

these stresses to be negligible.⁵ An explicit, though complicated, exact solution is available for the semi-infinite domain problem, see King and Cocco (2001); we side-step the complications. We also ignore localised stresses around the excavation that might be introduced by excavation supports⁶.

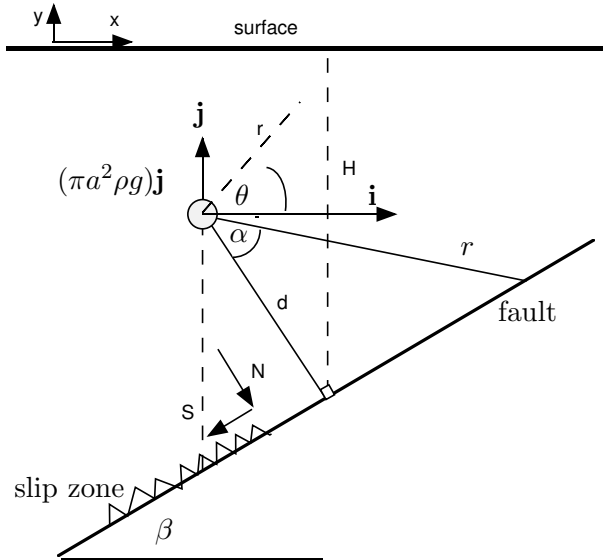


Figure 1: Tunnel geometry

The relevant result for the stress due to the concentrated point force \mathbf{P} as in (3.9) in an infinite elastic medium with Poisson ratio ν is given in Timoshenko and Goodier (1970), page 129. With respect to polar coordinates (r, θ) centred on the excavation with $\theta = 0$ in the \mathbf{i} direction as shown in Figure 1

$$\begin{aligned}\tau'_{rr} &= \frac{P}{4\pi}(3 + \nu)\frac{\sin \theta}{r}, \\ \tau'_{\theta\theta} &= -\frac{P}{4\pi}(1 - \nu)\frac{\sin \theta}{r}, \\ \tau'_{r\theta} &= \frac{P}{4\pi}(1 - \nu)\frac{\cos \theta}{r}.\end{aligned}$$

⁵The normal and tangential stresses at the surface are of order $(a/H)^2 = \epsilon(d/H)$. We keep terms of order ϵ but neglect terms of order $\epsilon(d/H)$.

⁶The effect of such supports may be studied by appending appropriate potential solutions

Our concern is with stress levels along the fault along which

$$\theta = 3\pi/2 + \beta + \alpha, \quad -\pi/2 < \alpha < \arctan(H/(d \sin \beta)), \quad r = d/\cos \alpha.$$

Also, expressed in polar co-ordinates, the stress distribution due to gravity at a point at depth h below the surface is

$$\tau_{rr}^0 = -\rho gh \sin^2 \theta, \quad \tau_{\theta\theta}^0 = -\rho gh \cos^2 \theta, \quad \tau_{\theta r}^0 = -\rho gh \sin \theta \cos \theta.$$

Using the above point force solution the shear stress S and normal force N acting on the fault as a function of position along the fault can be determined. We obtain

$$\frac{S}{|N|} = \frac{U}{V} \tan \beta, \quad (3.10)$$

where

$$\frac{U}{V} = 1 - \frac{\epsilon \cos \alpha [(1 + \nu) \cos \alpha \sin 2(\alpha + \beta) + (1 - \nu) \sin \alpha]}{2(1 - \frac{d}{H} \tan \alpha \sin \beta) \cos \beta \sin 2\beta} + \mathcal{O}(\epsilon^2), \quad (3.11)$$

and the dimensionless groups are

$$\epsilon = \frac{a^2}{Hd} \ll 1, \quad \frac{d}{H}.$$

The angles (β, α) specify the orientation of the fault and locations along the fault. Slip will occur along the fault if

$$S/|N| > \mu = \tan \beta_0,$$

where μ, β_0 are the coefficient of friction and angle of friction associated with the rock. Thus we have:

$$\text{the slip condition,} \quad \frac{U}{V} > \frac{\tan \beta_0}{\tan \beta}. \quad (3.12)$$

In the absence of the excavation ($\epsilon = 0$) this gives $\beta > \beta_0$. Our concern is with situations in which the fault angle is (marginally) sub-critical before the excavation is dug (so $\beta < \beta_0$) but the fault may be triggered by the presence of the excavation. The slip condition is plotted as a function of location α along the fault in Figure 2. It can be seen that slip occurs over the range $\alpha_1 < \alpha < \alpha_2$, where $-\beta_0 < \alpha_1 < 0$ i.e. the slip occurs in a zone further down the fault than the point nearest to the excavation, but above the location vertically below the excavation on the fault, see Figure 2. We will refer to this as the deep fault zone.

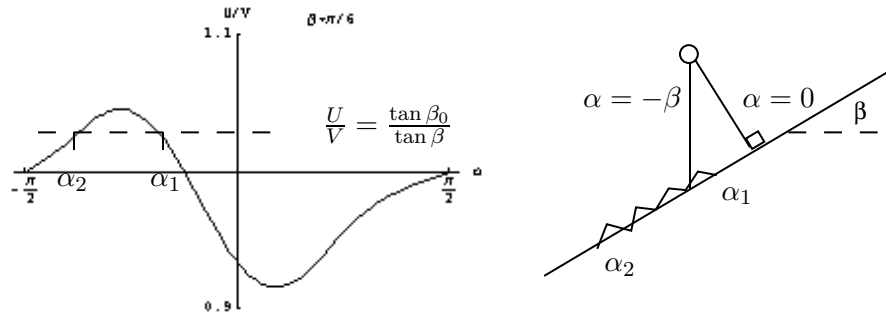


Figure 2: Fault slip due to an excavation above a fault. Slip occurs between $\alpha_2 < \alpha < \alpha_1$ where $\frac{\tan \beta_0}{\tan \beta} = \frac{U(\alpha)}{V(\alpha)}$. The parameters are $\beta = \pi/6, \nu = 0.25, d/H = 0.01, \epsilon = 0.1$. Note that $\alpha_1 > -\pi/6$ in this case.

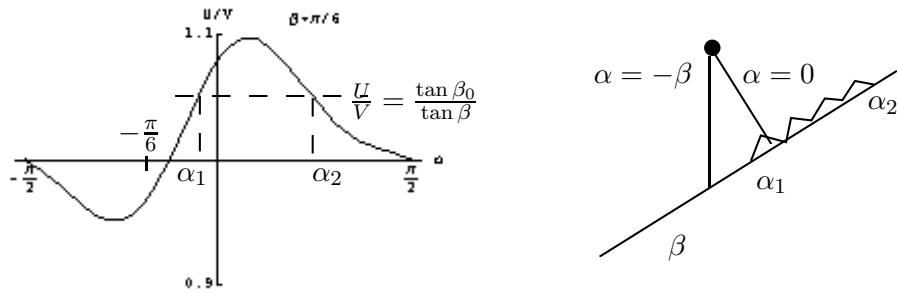


Figure 3: Fill-in effects with $\rho_1 > \rho$. Slip occurs between α_1 and α_2 where $\frac{\tan \beta_0}{\tan \beta} = \frac{U(\alpha)}{V(\alpha)}$. The parameters are $\beta = \pi/6, \nu = 0.25, d/H = 0.01, \bar{\epsilon} = 0.1$.

3.1.1 Fill in effects

One might well wonder if the filling in of the excavation with heavy material, with density $\rho_1 > \rho$, could stabilise a fault. The point force in this case is of strength

$$\mathbf{P} = -\rho g \pi a^2 \left(\frac{\rho_1}{\rho} - 1 \right) \mathbf{j} = P \mathbf{j},$$

so that the results (3.11, 3.12) go through with ϵ replaced by $-\bar{\epsilon}$ where $\bar{\epsilon} = \epsilon \left(\frac{\rho_1}{\rho} - 1 \right)$. Although the slip is stabilised in the deep fault zone, slip now occurs in the shallow fault zone, see Figure 3.

3.2 Fault slip due to a surface excavation or structure above a fault

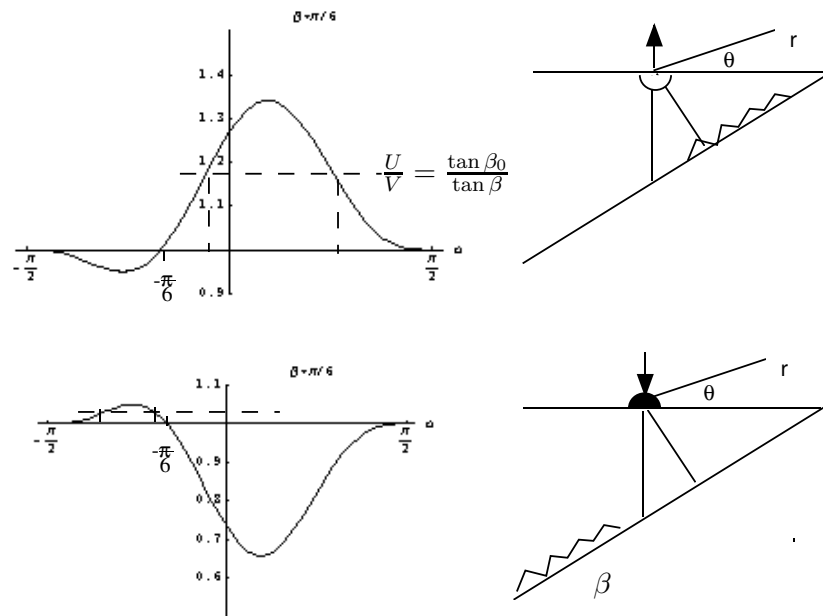


Figure 4: Upper Figures: a surface excavation. The parameters are $\beta = \pi/6, \nu = 0.25, \epsilon_s = 0.2$. Lower Figures: an erected building. The parameters are $\beta = \pi/6, \nu = 0.25, \bar{\epsilon}_s = 0.2$.

We will apply the result for the stress due to a concentrated point force magnitude P in the \mathbf{j} direction acting on a horizontal straight boundary of a semi-infinite plate. Adapted to the co-ordinate system used here, see Figure 4, the result of Timoshenko and Goodier (1970) p 98 is

$$\tau'_{rr} = -\frac{2P}{\pi r} \sin \theta, \quad \tau'_{\theta\theta} = 0, \quad \tau'_{r\theta} = 0.$$

The surface is traction free except at $r = 0$ where the point force acts. Interestingly the stress distribution is independent of the Poisson ratio ν . It can be derived from the potential

$$\phi = \frac{P}{\pi} r \theta \cos \theta.$$

In this application

$$\theta = \frac{3\pi}{2} + \beta + \alpha, \quad -\frac{\pi}{2} < \alpha < \frac{\pi}{2} - \beta.$$

For an excavation on the surface,

$$\mathbf{P} = P\mathbf{j} = \frac{\pi a^2}{2} \rho g \mathbf{j}.$$

The force P acts vertically upwards on the surface of the domain, see Figure 4. The shear and normal forces acting on the fault are straightforwardly calculated to again give the form

$$\frac{S}{|N|} = \left(\frac{U}{V} \right) \tan \beta, \quad (3.13)$$

where in this case

$$\frac{U}{V} = 1 + \frac{\epsilon_s \cos^3 \alpha \sin(\alpha + \beta)}{\cos^2 \beta \sin \beta} + \mathcal{O}(\epsilon_s^2), \quad \epsilon_s = \left(\frac{a}{d} \right)^2. \quad (3.14)$$

Thus again the fault slips at locations α determined by the fault slip condition (3.12) (but of course with altered values of U/V), which is plotted in Figure 4. Slip now occurs in the shallow fault zone. On the same figure we also observe the effect of surface loading; a fill in using material of density ρ_1 , where $\rho_1 > \rho$, or by a building of average density ρ_1 . Then

$$P = -\frac{\pi a^2}{2} g \left(\frac{\rho_1}{\rho} - 1 \right) \text{ (fill in),}$$

$$P = -\frac{\pi a^2}{2} g \rho_1, \quad (\text{building}),$$

and ϵ_s is replaced by $-\bar{\epsilon}_s$ where $\bar{\epsilon}_s = \epsilon_s(\rho_1/\rho - 1)$ and $\bar{\epsilon}_s = \epsilon_s \rho_1/\rho$ respectively. In this case slip can occur in the deep fault zone.

It is interesting to compare the effects of excavations deep within the Earth with surface excavations as seen in Figures 2 and 4. In the deep excavation case slip occurs in the deep fault zone, whereas in the surface excavation case the slip zone is shallow. Evidently surface effects play an increasingly important role as $d/H \rightarrow 0$ and this displays itself in the location of the slip zone. To explore the transition we would need to use the point force solution on the half plane which is available, see King and Cocco (2000), but is complex. This issue could be examined in subsequent work.

3.3 Fault slip due to an excavation below a fault

The above results carry across to the situations corresponding to excavations and fill ins below the fault. These results are displayed in Figure 5. Note that an excavation below the fault can result in slippage deep down, whereas a fill in with density $\rho_1 > \rho$ is likely to cause slippage in the shallow fault zone. An excavation on the surface can induce shallow slip whereas a fill in on the surface can help stabilise the fault. The relevant equations are:

excavation below the fault :

$$\frac{U}{V} = 1 + \frac{\epsilon \cos \alpha [(1 + \nu) \cos \alpha \sin 2(\beta - \alpha) - (1 - \nu) \sin \alpha]}{2(1 - \frac{d}{H} \tan \alpha \sin \beta) \cos \beta \sin 2\beta},$$

fill in below the fault :

$$\frac{U}{V} = 1 - \frac{\bar{\epsilon} \cos \alpha [(1 + \nu) \cos \alpha \sin 2(\beta - \alpha) - (1 - \nu) \sin \alpha]}{2(1 - \frac{d}{H} \tan \alpha \sin \beta) \cos \beta \sin 2\beta},$$

surface excavation :

$$\frac{U}{V} = 1 + \frac{\epsilon_s \cos^3 \alpha \sin(\beta - \alpha)}{\cos^2 \beta \sin \beta},$$

surface structure :

$$\frac{U}{V} = 1 - \frac{\bar{\epsilon} \cos^3 \alpha \sin(\beta - \alpha)}{\cos^2 \beta \sin \beta}.$$

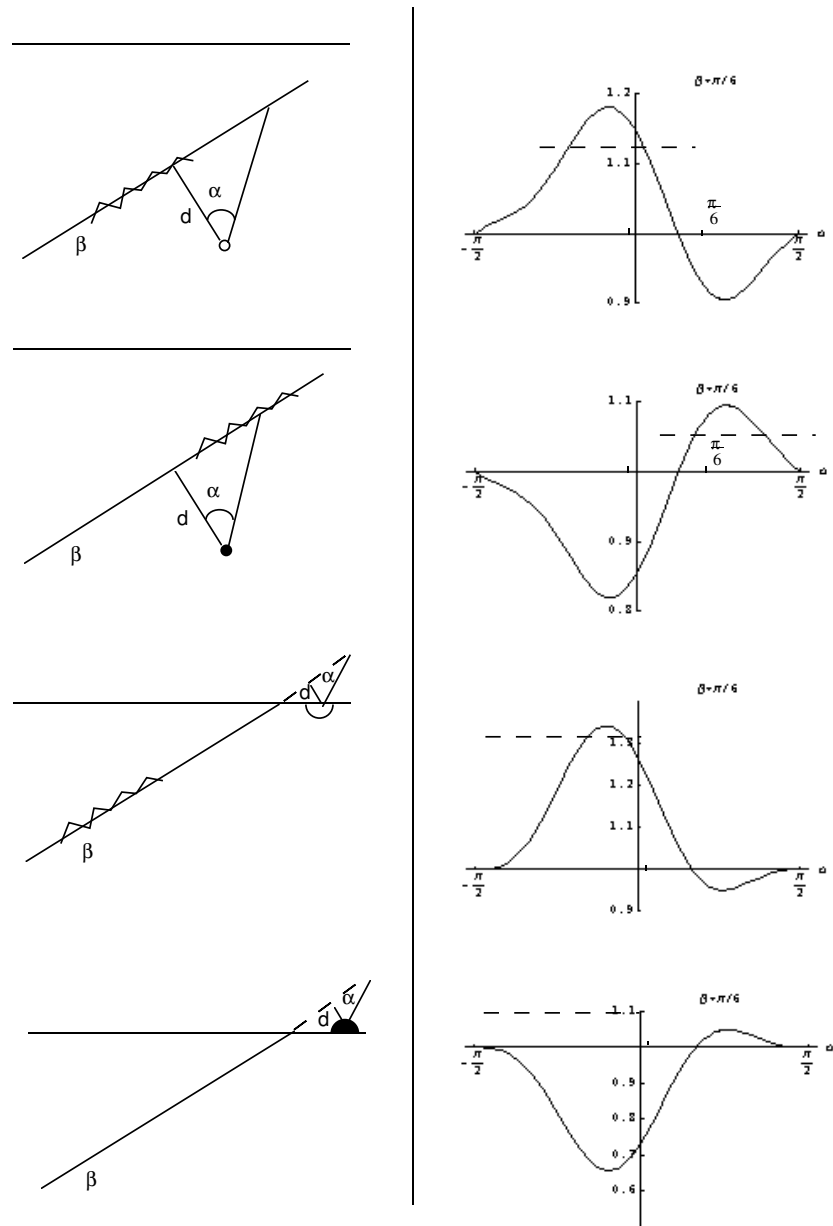


Figure 5: Upper Figures: deep excavations and fill ins under a fault. Lower Figures: excavations and a fill ins on the surface. In all cases $\frac{U}{V} > \frac{\tan \beta_0}{\tan \beta}$ is the slip condition. The dimensionless parameters are $\beta = \pi/6$, $\nu = 0.25$, $\epsilon = \frac{a^2}{Hd}$ and $\bar{\epsilon} = \epsilon(\frac{\rho_1}{\rho} - 1)$ or $\bar{\epsilon} = \epsilon \frac{\rho_1}{\rho}$ with $\epsilon = \bar{\epsilon} = 0.2$. Note that the portion of the U/V curves to the right of $\alpha = \beta - \pi/2$ correspond to locations outside the physical domain and so are not relevant.

In comparison with an excavation above a fault as described in Figure 2, for an excavation below a fault slip occurs in a zone further up the fault than the point of nearest approach ($\alpha = 0$) but below the location vertically above the excavation on the fault ($\alpha = \beta$).

3.4 Follow-up work

The above represents an attempt to understand the fault slip problem in simple circumstances.

Evidently solutions can be combined so that a complex (but strictly two-dimensional) arrangement of excavations can be examined, providing due care is taken with the interactions.

In the ambient stress, only the solution for $k = 0$ was considered. It would be important in follow-up work to consider the effect of k in the range $0 < k \leq 1$ on fault slip.

The solution for a point force in an infinite plane was used to investigate the effect of an excavation for deep excavations because surface effects can then be neglected. For excavations near the surface the point force solution in a half-plane would have to be used which is more complex (King and Cocco, 2000). This solution would also allow us to explore the transition from a deep excavation to a surface excavation.

The effect on the fault of localised stresses around the excavation (Jaeger and Cook, 1969) was neglected. These effects may be larger than the "buoyancy" effects due to the excavation of rock, especially for excavations close to the fault, and should be included in follow-up work. The relative importance of the localised stress effects and the buoyancy effects should be investigated.

The extension to three dimensions is also straightforward in theory but the Green's functions required are not so easy to work with and useful analytic results are unlikely.

Of course once slip occurs, cuts need to be introduced with the displacements across the cut prescribed by some theory/empirical result. The resulting slip may stabilise the fault or leave the fault in a critical state (most likely). In any case, in theory at least the determination of the stress field is straightforward *providing the slip model can be trusted*; the present models do not seem adequate.

4 Numerical and analytic solutions available for mining problems

This section provides a very brief survey of some representative techniques that have been applied to the analysis of stress changes induced by mining excavations. These include the use of analytical solutions, generally borrowed from mechanical engineering problems, of holes in elastic plates or other simple structures. In the important case of so-called tabular mining problems, where a thin seam or reef deposit is extracted, the excavation shape can be approximated as a crack with an irregular outline and with the crack faces allowed to interpenetrate one another to accommodate the effect of the compressive stress environment in which the excavation is created. An early example of this form of approximation is given by Hackett (1959) for the analysis of coal mining problems. A number of additional two-dimensional problems were analysed by Salamon (1968), using complex variable solution techniques based on the work of Muskhelishvili, 1963.

Although the available analytical methods provide great insight into the canonical nature of some basic problems of stress concentration near the edges of mine openings, it is apparent that for engineering design purposes, it is generally necessary to obtain more detailed insights into the effects of particular excavation configurations on surrounding fault structures or other excavations. In this respect, traditional techniques such as the Finite Element Method (FEM) are somewhat cumbersome due to the infinite or semi-infinite nature of the mining region and the need to cover the entire volume with a computational mesh unless special infinite elements are used. This has given some impetus to the use of boundary integral techniques where only the significant excavation surfaces need to be defined in the problem specification. The major disadvantage of the boundary integral approach is the need to have a closed form fundamental solution (Greens function) that is usually only available for a simple elastic material model. A particular version of this approach was proposed by Salamon (1963) for the analysis of stress concentrations arising from tabular mining operations in an elastic host material. Salamon initially termed the method the Face Element Principle but this has subsequently become known as the Displacement Discontinuity Method (DDM). An exposition of the basic method is given by Crouch and Starfield (1983) and has found specialised application in the routine solution of tabular gold, coal and platinum mining problems (Salamon et al., 1964, Plewman et al., 1969), particularly in South Africa. The DDM has also found applications in attempts to model earthquake slip

processes (see, for example, Ben-Zion and Rice, 1993). Further extensions to the method can be developed to model inelastic fracture initiation near the highly stressed edges of tabular mine excavations (Napier and Malan, 1997).

It is important to note that the displacement discontinuity method (DDM) can be extended to analyse problems of dynamic fault slip that are of great interest in the fields of earthquake engineering and seismology (see, for example, Aki and Richards, 1980, Scholz, 2002). However, a number of difficult numerical challenges arise in applying the DDM to elastodynamic fault slip problems that require attention to the treatment of multiple time and length scales and to issues of numerical stability. This suggests that it may be fruitful to consider "hybrid" models that embrace both discontinuity structures and particle model concepts such as the so-called smoothed particle hydrodynamics (SPH) technique.

5 Conclusions and recommendations

In the above we have attempted to provide a considered, but necessarily brief, survey of relevant physical models and numerical approaches that have been used, or may be used, to shed light on this very difficult problem. We have also attempted to give a careful treatment of one small aspect of the problem; the effect of excavations and possible structures on an existing fault. The approach employed may provide useful practical information for slip management and may be usefully extended. The work is continuing.

A very profitable route for dynamic fracture modelling might be the development of hybrid models that embrace both the boundary integral ideas and the particle model concepts of smoothed particle hydrodynamics.

Acknowledgements

Members of the Study Group that contributed to the discussions were Alistair Fitt, Robert Sarricino, Gazanfer Unaland Masood Khaliq. We acknowledge their contribution to the understanding of the problem. D. P. Mason acknowledges support of this work under the National Research Foundation of South Africa grant number 2053745.

References

- Aki, K. and Richards, P.G. (1980). *Quantitative seismology*, W.H. Freeman and Company, New York.
- Ben-Zion, Y. and Rice, J. R. (1993). Earthquake failure sequences along a cellular fault zone in a three-dimensional elastic solid containing asperity and non-asperity regions, *J. Geophys. Res.*, **98**, 14109-14131.
- Sawley, M.L., Cleary, P.W. and Ha, J. (2000). Using smoothed particle hydrodynamics for industrial flow simulations, EPFL, Supercomputing Review, **12**, 3-8.
- Crouch, S.L. and Starfield, A.M. (1983). *Boundary element methods in solid mechanics*, George Allen & Unwin, London.
- Dieterich, J.H. (1966). Implications of fault constitutive properties for earthquake prediction. *Proc. Nat. Acad. Sci. USA* **93**, 3787-3794.
- Dyskin, A.V. and Galybin, A.N. (2004). Solutions for dilating shear cracks in an elastic plane, *Int. J. Fracture*, **109**, 325-344.
- Gibowicz, S.J. and Lasocki, S. (2000). Seismicity induced by mining: Ten years later, *Advances in Geophysics*, **44**, 39-167.
- Hackett, P. (1959). An elastic analysis of rock movements caused by mining, *Trans. Instn. Min. Engrs*, **118**, 421-435.
- Jaeger, J.C. and Cook, N.G.W. (1969). *Fundamentals of Rock Mechanics*, Methuen, London, pp 236-241 and 355-357.
- King, C.G. and Cocco, M. (2000). Fault interaction by elastic stress changes: New clues from earthquake sequences, *Advances in Geophysics*, **44**, 1-96.
- Monaghan, J.J. (1992). Smoothed particle hydrodynamics, *Annu. Rev. Astrophys.* **30**, 543-74.
- Muhlhaus. H. (1999). *Non-classical elastic models: Continuum models for materials with microstructure*. J. Wiley, New York.
- Mushelishvili, N.I. (1963). *Some Basic Problems of the Mathematical Theory of Elasticity*, Nordhoff, Groningen.
- Napier, J.A.L. and Malan, D.F. (1997). A viscoplastic discontinuum model of time-dependent fracture and seismicity effects in brittle rock, *Int. J. Rock Mech. Min. Sci.*, **34**, 1075-1089.
- Panza, G. F., Romanelli, F. and Vaccari, F. (2000). Seismic wave propaga-

tion in heterogeneous anelastic media: Theory and applications to seismic zonation, *Advances in Geophysics*, **43**, 1-93.

Plewman, R. P., Deist, F. H. and Ortlepp, W. D. (1969). The development and application of a digital computer method for the solution of strata control problems, *J. S. Afr. Inst. Min. Metall.*, **70**, 33-44.

Salamon, M.D.G. (1968). Two-dimensional treatment of problems arising from mining tabular deposits in isotropic or transversely isotropic ground, *Int. J. Rock Mech. Min. Sci.*, **5**, 159-185.

Salamon, M.D.G. (1963). Elastic analysis of displacements and stresses induced by the mining of seam or reef deposits, *J. S. Afr. Inst. Min. Metall.*, **64**, 128-149.

Salamon, M.D.G., Ryder, J.A. and Ortlepp, W.D. (1964). An analogue solution for determining the elastic response of strata surrounding tabular mining excavations, *J. S. Afr. Inst. Min. Metall.*, **64**, 115-137.

Scholz, C.H. (2002). *The mechanics of earthquakes and faulting*, Cambridge University Press, Cambridge, 2nd edition.

Timoshenko, S. P. and Goodier, J.N. (1970). *Theory of Elasticity*, McGraw Hill, New York, pp 13-133.